Debattisti et al., http://www.jcb.org/cgi/content/full/jcb.201306121/DC1

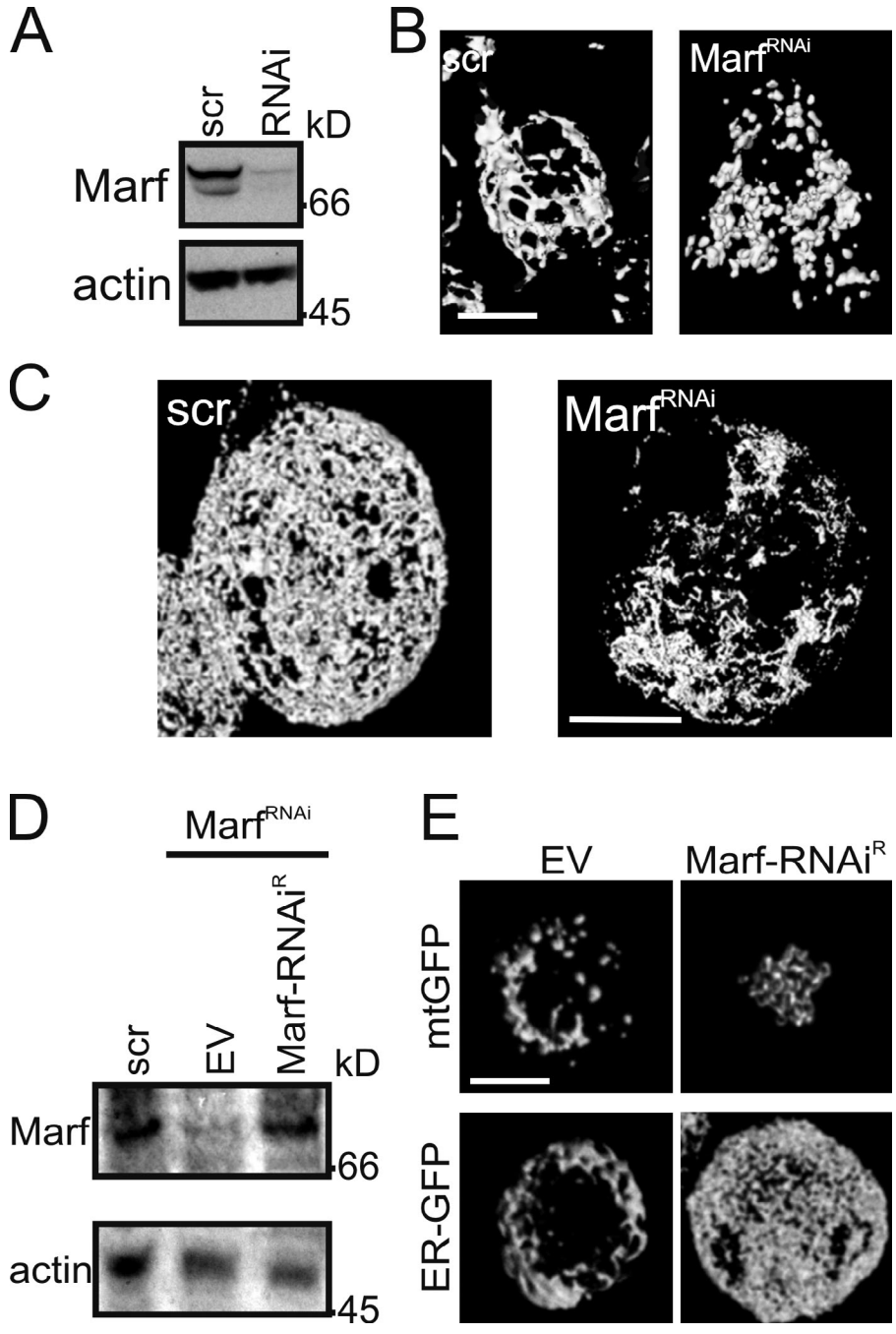

Figure S1. **Efficient Marf^{RNAi} alters mitochondrial and ER morphology.** (A) Equal amounts of protein (50 µg) from S2R+ cells treated for 96 h with the indicated dsRNA were separated by SDS-PAGE and immunoblotted with the indicated antibodies. (B) Surface-rendered 3D reconstructions of confocal z stacks of S2R+ cells treated with the indicated dsRNA for 96 h and stained with 20 nM tetramethylrhodamine methyl ester. (C) Surface-rendered 3D reconstructions of confocal z stacks of S2R+ cells transfected with the ER marker Atl^{TM}-GFP and the indicated dsRNA for 96 h. (D) Equal amounts of protein (50 µg) from S2R+ cells treated with the indicated dsRNA and transfected as indicated were separated by SDS-PAGE and immunoblotted with the indicated antibodies. (E) Surface-rendered 3D reconstructions of confocal z stacks of S2R+ cells treated with the indicated dsRNA and transfected as indicated. EV, empty vector; scr, scrambled. Bars: (B and E) 10 µm; (C) 8 µm.

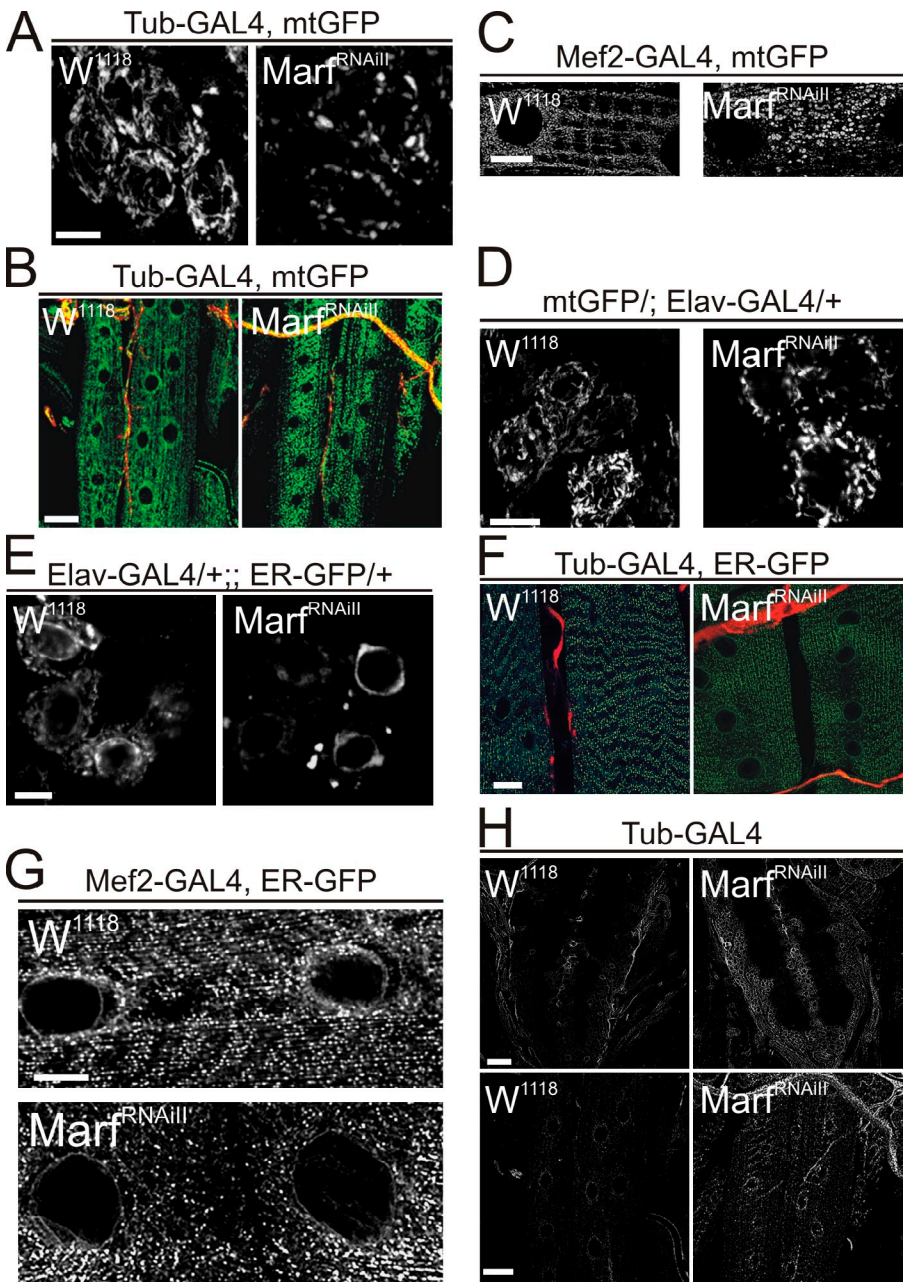

Figure S2. **ER and mitochondrial defects are found in a second Marf^{RNAi} line.** (A) Maximum projections of confocal stacks of mtGFP in neuronal cell bodies acquired in tubulin-Gal4, UAS-mtGFP /+ (W1118), and UAS-Marf^{RNAi}/+; tubulin-Gal4, UAS-mtGFP /+ (Marf$^{RNAi-II}$) larvae. (B) Maximum projections of confocal stacks of mtGFP from muscles 6 and 7 labeled with α-HRP (red) acquired from larvae of the same genotype as in A. mtGFP is pseudocolored in green. (C) Representative confocal images of mtGFP in body wall muscles of Mef2-Gal4, UAS-mtGFP/+ (W1118), and UAS-Marf^{RNAi}/+; Mef2-Gal4, UAS-mtGFP/+ (Marf$^{RNAi-II}$) larvae. (D) Maximum projections of confocal stacks of mtGFP in neuronal cell bodies acquired in UAS-mtGFP/+; Elav-Gal4/+ (W1118) and UAS-mtGFP/ UAS-Marf^{RNAi}; Elav-Gal4/+ (Marf$^{RNAi-II}$) larvae. (E) Representative confocal images of ER-GFP in neuronal cell bodies of Elav-Gal4/+;; UAS–ER-GFP/+ (W1118) and Elav-Gal4/+; UAS-Marf^{RNAi}/+; UAS–ER-GFP/+ (Marf$^{RNAi-II}$) larvae. (F) Representative confocal images of ER-GFP in muscles 6 and 7 (NMJs labeled with α-HRP, red) of tubulin-Gal4, UAS–ER-GFP/+ (W1118) and UAS-Marf^{RNAi}/+; tubulin-Gal4, UAS–ER-GFP/+ (Marf$^{RNAi-II}$) larvae. (G) Representative confocal images of ER-GFP in muscle 7 of Mef2-Gal4, UAS–ER-GFP/+ (W1118) and UAS-Marf^{RNAi}/+; Mef2-Gal4, UAS–ER-GFP/+ (Marf$^{RNAi-II}$) larvae. (H) Representative confocal images of ventral ganglion (top) and muscle walls (bottom) of tubulin-Gal4/+ (W1118) and UAS-Marf^{RNAi}/+; tubulin-Gal4/+ (Marf$^{RNAi-II}$) larvae labeled with α-BiP. Tub, tubulin. Bars: (A–E, G, and H) 10 µm; (F) 20 µm.

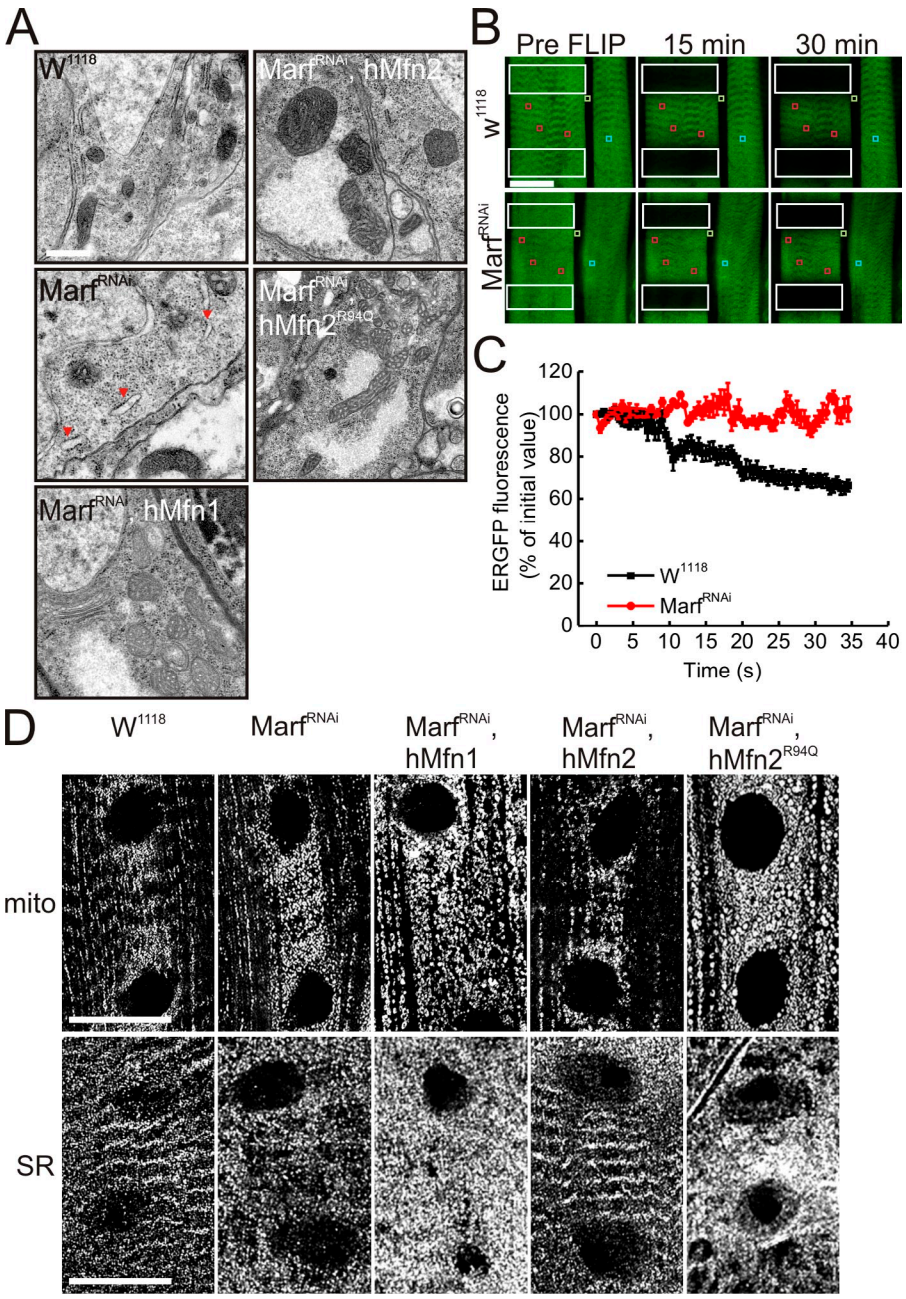

Figure S3. **Marf ablation causes ER dilation and reduces SR luminal continuity.** (A) Electron microscopy images of neuronal cell bodies of Elav-Gal4/+ larvae of the indicated genotype. Arrowheads indicate ER. Bar, 5 µm. (B) Representative confocal microscopy images of muscle walls from FLIP experiments. Repetitive photobleaching of two ROI (white outline boxes) in Mef2-Gal4/ + (W1118) and Mef2-Gal4/UAS-Marf^{RNAi} (Marf^{RNAi}) muscles expressing GFP-KDEL was performed. Fluorescence loss was analyzed in three independent regions of the muscle (red outline boxes). One ROI was chosen on an adjacent unbleached muscle as a control (light blue outline box). A fifth ROI was chosen for background subtraction (yellow outline box). Bar, 20 µm. (C) ER-GFP fluorescence recordings from real-time FLIP in muscles walls of Mef2-Gal4/ + (W1118) and Mef2-Gal4/UAS-Marf^{RNAi} (Marf^{RNAi}) larvae. Data represent means ± SEM of three independent experiments. (D) Confocal images of body wall muscles of MHC-Gal4/+ larvae of the indicated genotype labeled with α-ATP synthase, subunit α (mito) or with α-atlastin (SR). Bars, 10 µm.